Acta Derm Venereol (Stockh) 1999; 79: 54–61

In vivo Detection of Basal Cell Carcinoma using Imaging Spectroscopy

ANN-MARIE WENNBERG[1], FREDRIK GUDMUNDSON[4], BO STENQUIST[3], ANNIKA TERNESTEN[2], LENA MÖLNE[1], ARNE ROSÉN[4] and OLLE LARKÖ[1]

Departments of [1]Dermatology, [2]Pathology, Göteborg University, Sahlgrenska University Hospital, [3]Department of Surgery, Lundby Hospital and [4]Department of Physics Chalmers University of Technology and Göteborg University, Göteborg, Sweden

Photodynamic therapy has become an interesting alternative to conventional therapy for basal cell carcinomas. Delta-aminolevulinic acid is a precursor in the biosynthesis of protoporphyrin IX that accumulates to a large extent in tumour tissue. We have compared *in vivo* protoporphyrin IX fluorescence with the extent of basal cell carcinomas on the face, trunk and thigh determined by histological mapping in 30 lesions in 22 patients. A new non-laser based set-up was used to record the fluorescence images. Delta-aminolevulinic acid was applied for 4 h inducing high concentrations of protoporphyrin IX. Routine vertical histological sections and Mohs micrographic surgery were used to map the extent of the tumours. In 50% of lesions we found a good correlation between the fluorescence imaging and histological mapping. In 23% the correlation was partial. In the other lesions we found no correlation at all. This method may be used to delineate basal cell carcinomas more accurately than current methods. *Key words: delta-aminolevulinic acid; fluorescence; Mohs micrographic surgery; protoporphyrin.*

(Accepted July 15, 1998.)

Acta Derm Venereol (Stockh) 1999; 79: 54–61.

A.-M. Wennberg, Department of Dermatology, Sahlgrenska University Hospital, SE-41345 Göteborg, Sweden.

Basal cell carcinoma (BCC) is the most common skin cancer among people with skin types I – III. The most common treatment modalities are surgery, cryosurgery, curettage and electrodesiccation. The recurrence rate for primary tumours with these procedures is 5 – 10% within 5 years (1)

Photodynamic therapy (PDT) has in recent years become an interesting alternative method of treating non-melanoma skin tumours (2, 3). The most promising PDT procedure for dermatological use is topical application of delta-aminolevulinic acid (ALA) with subsequent irradiation with red light centred around 635 nm (3, 4). The relatively small ALA molecules penetrate the skin and are taken up by the cells. ALA is a precursor in the biosynthesis of haeme and the photosensitizer protoporphyrin IX (Pp IX) is therefore formed in the cells. It has been found that Pp IX accumulates to a larger extent in tumour tissue than in normal tissue (5 – 8). When cells containing Pp IX are irradiated with light centred around 635 nm, tumour cells are selectively killed. Pp IX also has absorption peaks at shorter wavelengths, but red light is the best choice for PDT as this light has a good depth of penetration in human skin (9). It has been shown that PDT with ALA is safe and gives cosmetically superior results. PDT has been evaluated clinically in several studies (3, 5, 10, 11).

In the present study, we used a simple and inexpensive technical device for excitation of Pp IX. The fluorescence images were recorded digitally. In order to evaluate the efficacy of the set-up, we studied the correlation between the lateral extent of BCCs as given by histopathological analysis and the *in vivo* fluorescence images. When evaluating the fluorescence of aggressive and morpheiform BCCs on the face, Mohs micrographic surgery was performed as a control (12).

MATERIALS AND METHODS

Patients

The study was carried out at the Department of Dermatology, Sahlgrenska Hospital, Göteborg University, Sweden, and was approved by the local ethics committee. A total of 22 patients (8 men and 14 women; mean age 65 years, range 45 – 87) with 30 BCCs (13 SBCCs, 11 MBCCs and 6 NBCCs) were investigated. All clinically visible lesions were measured prior to treatment. All tumours were histopathologically verified. The fluorescence imaging of the initial 5 patients was made with an intensified charge coupled device (ICCD) and the following 17 patients were imaged with thermoelectrically cooled charge coupled device (TE/CCD). Mohs fresh frozen tissue technique was performed afterwards.

ALA treatment

A freshly made cellulose gel (sodium carboxymethyl cellulose in sterile water) containing 20% delta-aminolevulinic acid hydrochloride (Porphyrin Products, Logan, Utah) was applied to the skin for 4 h before fluorescence imaging was carried out. The ALA gel was occluded under a plastic film (Tegaderm®, 3M).

Digital fluorescence imaging

The equipment used to image the fluorescence of Pp IX in the skin consisted of a light source and a charge coupled device (CCD) with a Nikon UV quartz 4.5 lens, f = 105 mm. The fluorescence images were recorded with 16384 intensity level resolution. For the first 12 investigated lesions an intensified CCD camera (Princeton Instruments ICCD, 384 × 578 pixels) was used and for the remaining investigations a non-intensified camera was used (Princeton Instruments TE/CCD, 384 × 578 pixels).

Both the camera and the light source were fitted with filters chosen to match the emission and absorption of Pp IX. The filters and light source were also chosen so as to minimize fluorescence of other chemical substances in the skin. The light source was a mercury lamp fitted with a bandpass glass filter selecting wavelengths in the range 310 – 500 nm. The camera was fitted with a longpass filter only letting through light with wavelengths longer than 590 nm. The intensity of the light at the skin of the patient was approximately 0.5 mW/cm^2. The experimental set-up is shown in Fig. 1.

Whilst the fluorescence images were being recorded, the patient was either seated on a chair or lying on a couch. Care was taken to provide sufficient support for the patient to avoid movement during the exposure time. The plastic covering the area that had been exposed to the ALA gel was removed. The remaining ALA gel was wiped off with a paper tissue. The light from the filtered mercury lamp was centred on the area of interest. The homogeneity of the light intensity was checked by removing the filter from the camera and taking a picture of the area

 ISSN 0001-5555

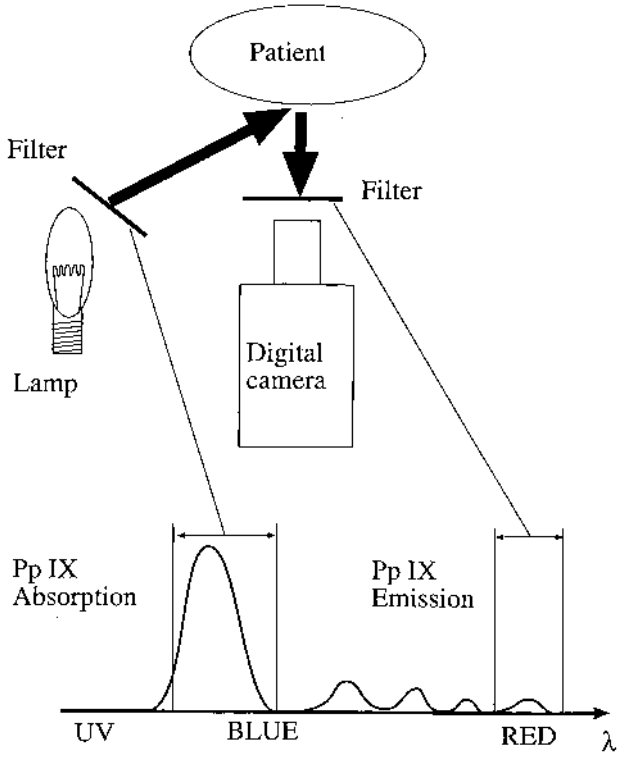

Fig. 1. Schematic overview of the experimental set-up for recording fluorescence images. The light from a filtered mercury lamp causes the Pp IX molecules to fluoresce red. This light is recorded with a filtered CCD camera. The spectra and approximate filter limits are shown in the lower part of the figure.

of interest. The directly reflected light was then stronger than the fluorescence light and the homogeneity of the intensity could be checked. The fluorescence images were recorded with the lights in the room switched off. The exposure time used for the images was 2 seconds.

The fluorescence images were analysed with a standard program that only handles images with 256 intensity levels. Therefore, the information in the original files had to be translated to 8-bit format. To minimize loss of information, the data in the range of zero to the maximal intensity level was recalculated to 256 intensity levels. The maximum intensity level in the original image varied from one image to the other due to variations in the light emitted from the imaged objects. The most important factors were the intensity of the incoming light and the distance between the camera and the imaged area. For the first 7 patients a single filtered mercury lamp was used and for the rest three lamps were placed around the camera. When the intensified camera was used the maximum intensity level also depended on the voltage applied to the microchannel plates.

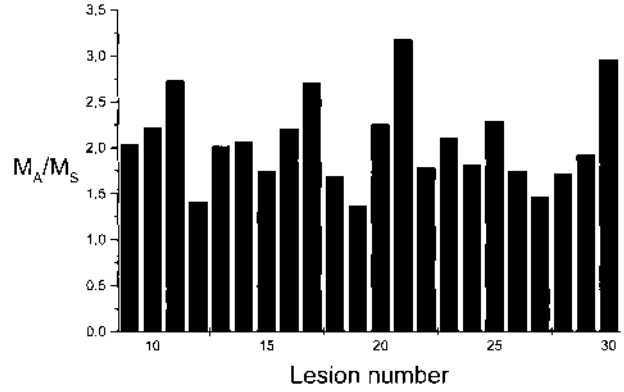

Fig. 2. Ratio between the mean intensity in the ALA-treated area (M_A) and mean intensity in the non-treated surrounding skin (M_S).

Image normalization procedure

The fluorescence from the skin gives rise to an image that closely resembles a black and white photograph if displayed in gray scale. The region where the ALA has been applied appears brighter than the surrounding skin. Within the area where ALA has been applied there are brighter spots which in many cases correlate with tumour sites.

The average and standard deviation of the ALA-treated area and of the surrounding non-treated skin fluorescence is calculated. The mean intensity in the ALA-treated area and the non-treated area will be denoted M_A and M_S respectively in the following text and the corresponding standard deviations SD_A and SD_S. The ratio M_A /M_S is shown in Fig. 2 for all the investigated lesions which were excised and histologically mapped (no 9–30). This ratio (mean 2.07 ± SD 0.48) reflects the relative strengths of untreated skin and ALA-treated skin fluorescence. The ratio cannot be directly related to PpIX concentration as variations in illumination and quenching are not well controlled.

The mean ± SD for M_A −2 SD_A was 0.63 ± 0.083 and for M_A +2 SD_A 1.37 ± 0.083. These results are used to find appropriate levels for a colour scale that can be applied to all images. The intensity levels in the original images corresponding to M_A are shown in Tables I and II

Table I. *Lesions examined with biopsies or excisions*

Lesion	BCC type	Location	Histological examination	Clinical size (mm)	Histological size (mm)	Fluorescence size (mm)	Correlation	M_A Intensity	Fig.
1–6	SBCC	Back	Biopsies	10 × 20	–	9 × 7	–	–	
				12 × 30		15 × 29			3a
				14 × 10		3 × 3			3b
				10 × 30		13 × 16			
				Not visible		10 × 12			
				Not visible		9 × 9			
7–8	SBCC	Back	Biopsies	10 × 10	–	10 × 11	–	–	
				7 × 8		8 × 9			
9	SBCC	Left cheek	Excision	6 × 6	7 × 11	5 × 5	Partial	3091	
10	SBCC	Chest	Excision	7 × 15	12 × 19	11 × 19	Good	5242	3c
11	SBCC	Thigh	Excision	5 × 6	10 × 11	10 × 9	Good	4380	

SBCC: superficial basal cell carcinoma.

Table II. *Lesions examined with Mohs surgery*

Lesion number	BCC type	Location	Clinical size (mm)	Histological size (mm)	Fluorescence size (mm)	Correlation	M_A Intensity	Fig. no.
12	Primary SBCC	Back	8 × 17	12 × 8	10 × 6	Good	4640	
13	Primary MBCC	Right ala	10 × 10	10 × 17	10 × 16	Good	267	
14	Primary MBCC	Right cheek	15 × 10	10 × 10	10 × 10	Good	161	4a 4b
15	Primary MBCC	Right ala	4 × 4	12 × 13	–	No	432	
16	Primary MBCC	Right lower eyelid	10 × 7	12 × 11	10 × 9	Good	691	4c 4d
17	Recurrent NBCC	Corner of the right eye	6 × 4	1 × 1	–	No	262	4e 4f
18	Recurrent MBCC	Right lower eyelid	17 × 5	24 × 10	3 × 2	Partial	164	
19	Suspected SBCC	Left lower eyelid	4 × 4	–	–	No	139	
20	Recurrent NBCC	Corner of the right eye	7 × 7	0 × 0	0 × 0	Good	657	4g 4h
21	Recurrent NBCC	Left side of nose	15 × 15	20 × 20	6 × 10	Partial	227	
22	Primary MBCC	Nose tip	14 × 12	18 × 23	–	No	168	
23	Recurrent MBCC	Nose tip	10 × 10	14 × 15	1 × 1	Partial	369	
24	Recurrent NBCC	Corner of the left eye	4 × 4	4 × 7	6 × 9	Good	328	
25	Recurrent NBCC	Left cheek	11 × 13	3 × 5	–	No	496	
26	Recurrent MBCC	Right ear	15 × 25	14 × 20	14 × 22	Good	237	4i 4j
27	Primary MBCC	Left ala	11 × 9	10 × 8	5 × 5	Partial	349	
28	Primary MBCC	Left cheek	10 × 10	6 × 4	–	No	525	
29	Primary MBCC	Corner of the right eye	9 × 9	7 × 4	4 × 3	Good	349	4k 4l
30	Recurrent NBCC	Right ala	10 × 10	15 × 8	14 × 10	Good	402	

MBCC: morpheiform basal cell carcinoma; NBCC: nodular basal cell carcinoma; SBCC: superficial basal cell carcinoma.

(M_A intensity). This makes it possible to relate the intensities in the presented images to the intensity level in the original images. One intensity level is approximately 50 photons when the non-intensified CCD camera is used. Using the intensified CCD camera the approximate number of photons per intensity level is 5.

Fluorescence intensities below $M_A + 2SD_A$ are difficult to separate from variations of the fluorescence in the ALA-treated area. In most investigated lesions the variations in the ALA-treated area do not exceed 1.4 M_A. Therefore 1.4 M_A is chosen as a lower limit for the estimate of tumour extent. A colour scale is applied that gives information on the fluorescence intensity in the range 1.4 – 2 M_A. Below 1.4 M_A the image is represented in a gray scale. The upper limit of the intensity in the image is chosen to be 2 M_A as most data do not exceed this level.

Histopathological analysis

The BCCs presented in Table II were excised using Mohs fresh frozen tissue technique without prior knowledge of the fluorescence results. To determine the lateral extent of the tumours, the frozen tissue blocks were re-embedded in paraffin with the borders pushed back to the surface. From these paraffin blocks, 4 μm sections were cut from the surface down into the block at 3 – 4 levels. These sections, together with the primary frozen sections, gave a more precise picture of the vertical as well as lateral extent of the tumour. All microscopically verified tumour tissue was mapped in a separate chart for each excisional biopsy without knowledge of the fluorescence images. The tumour extent was inscribed with a black line in the photograph recorded before surgery. Due to the elasticity of the skin and changes in form we estimate the precision of this method of marking the tumour to be ±3 mm.

The SBCCs presented in Table I were not excised by Mohs surgery. A different technique was used to map the extent of the tumour. Each specimen was fixed in 10% formaldehyde solution, processed to paraffin blocks and stained with haematoxylin – eosin. The excisional biopsies were cut vertically in slices 1 – 2 mm thick. Sections 4 μm thick were obtained at 3 – 4 levels from each paraffin block. The histopathological mapping was inscribed on the digital images as short black lines.

Criterion for correlation

The correlation between fluorescence and histology is judged to be in one of the categories good, partial or no correlation. The correlation is judged to be good if the extent according to histological examination agrees within 3 mm in non-ulcerated skin. It is partial if there is a correspondence regarding the localization but not the extent.

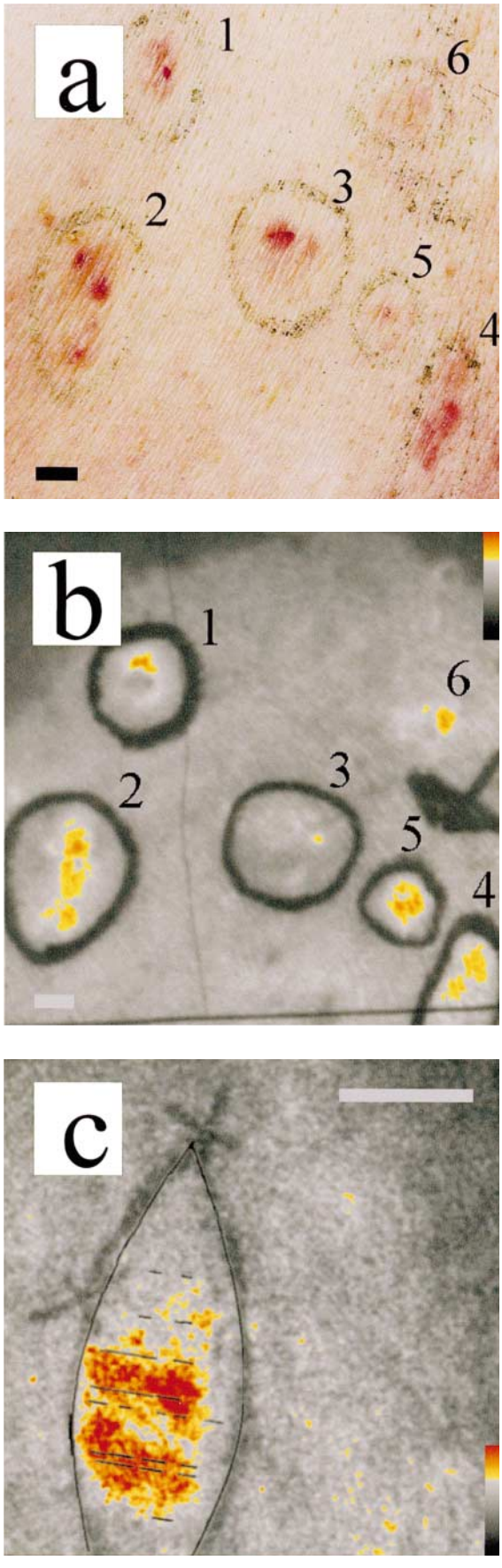

RESULTS

The results are presented in detail for all lesions in Tables I and II.

In this research, we used two types of digital devices to image the fluorescence. In lesions 1 – 12 (Tables I and II) we used an ICCD camera and in lesions 13 – 30 (Table II) we used a TE/CCD camera. We began the study with the more sensitive ICCD camera but we found that the intensity of the generated fluorescence was high enough to use a TE/CCD. The much better imaging properties of the TE/CCD made it more suitable for imaging tumours located on the face.

Lesions examined with biopsies or excisions (Table I)

Fig. 3a shows the photographic documentation and Fig. 3b the fluorescence imaging of SBCCs on a patient's back. Fig. 3c shows the fluorescence image of a clinically detected SBCC on a patient's chest.

Lesions examined with Mohs micrographic surgery (Table II)

All the lesions in Table II except number 12 were localized to the face and were growing aggressively. Some examples are shown below. Fig. 4a shows an MBCC on the right cheek. The high intensity fluorescence in Fig. 4b correlates well with the tumour extent except for ulcerated areas. Fig. 4c shows an MBCC on the right lower eyelid. The tumour extends in caudal direction, a feature also seen in the fluorescence image in Fig. 4d. In a small area of ulceration next to the lateral corner of the eye there is no fluorescence. Note that the eye is open in Fig. 4c and closed in Fig. 4d.

Fig. 4e shows a recurrent NBCC (arrow) in the corner of the right eye. In Fig. 4f a small spot was found by fluorescence imaging and confirmed by histopathology as an SBCC (encircled in Fig. 4e). The area surrounding the punch biopsy, indicated with arrows (in Figs 4e and f), did not exhibit any increased fluorescence, even though the histopathological analysis showed that there was residual tumour growth in the depth of the biopsy.

The patient in Fig. 4g was referred to surgery because a previous punch biopsy had shown recurrence of NBCC. The location of the punch biopsy is indicated with arrows in Figs. 4g

Fig. 3. (*a*) Photograph and (*b*) fluorescence image of a patient's back with several superficial BCCs. Areas 5 and 6 were identified as tumours only with the fluorescence imaging technique. The black circles and the black arrow in (*b*) were lines drawn on the skin with a pencil. The skin is stretched in (*a*) making the rings more oval than in (*b*). The encircled areas 1 – 4 are tumours that have been clinically diagnosed as SBCCs. Areas 5 and 6 were not identified as tumours before the fluorescence image was recorded. The photograph was taken the day after the fluorescence image was recorded and the areas have become red after the illumination. Punch biopsies confirmed the occurrence of SBCCs in these areas. Area 6 was encircled after the fluorescence picture (*b*) was taken. (*c*) Fluorescence image showing an SBCC located on the chest. The histopathological mapping was inscribed as short black lines. The colour bar relates the measured intensities with the colours. The ellipse-shaped black lines indicate the area that was removed by excision. The short parallel black lines within the ellipse show the extent of the tumour according to histopathological analysis. Scale bar 10 mm.

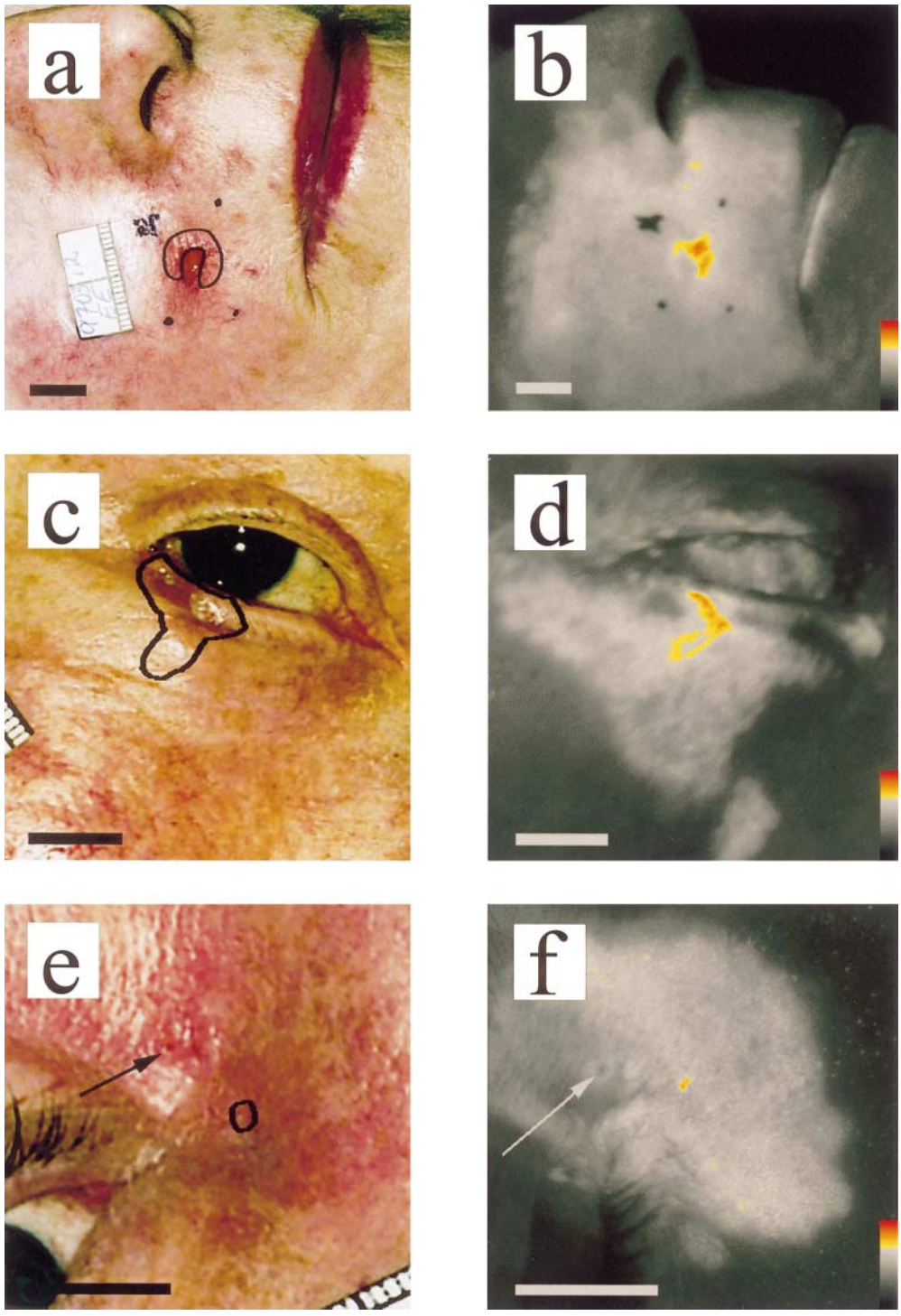

Fig. 4. Photographs and fluorescence images of lesions on various parts of the face. The patients were operated with Mohs fresh frozen tissue technique. The extent of the lesions as determined by histopathology is marked with black lines. The colour bar relates the measured intensities with the colours. Scale bar 10 mm.

and 4h. No tumour was found in the removed tissue when analysed. This correlates well with the fluorescence image in Fig. 4h. Figs. 4i and 4j show a recurrent MBCC on the right ear. Good correlation between fluorescence image and the histopathological judgement was seen. Figs. 4k and l show a primary MBCC in the corner of the right eye, also with good correlation between fluorescence and histopathology.

Correlation according to the threshold criteria

In 11/22 (50%) of lesions which were histologically mapped we found good correlation (overlay) between fluorescence detected area and the histopathological mapping. In 5/22 lesions (23%) we found partial correlation and in 6/22 (27%) there was no correlation.

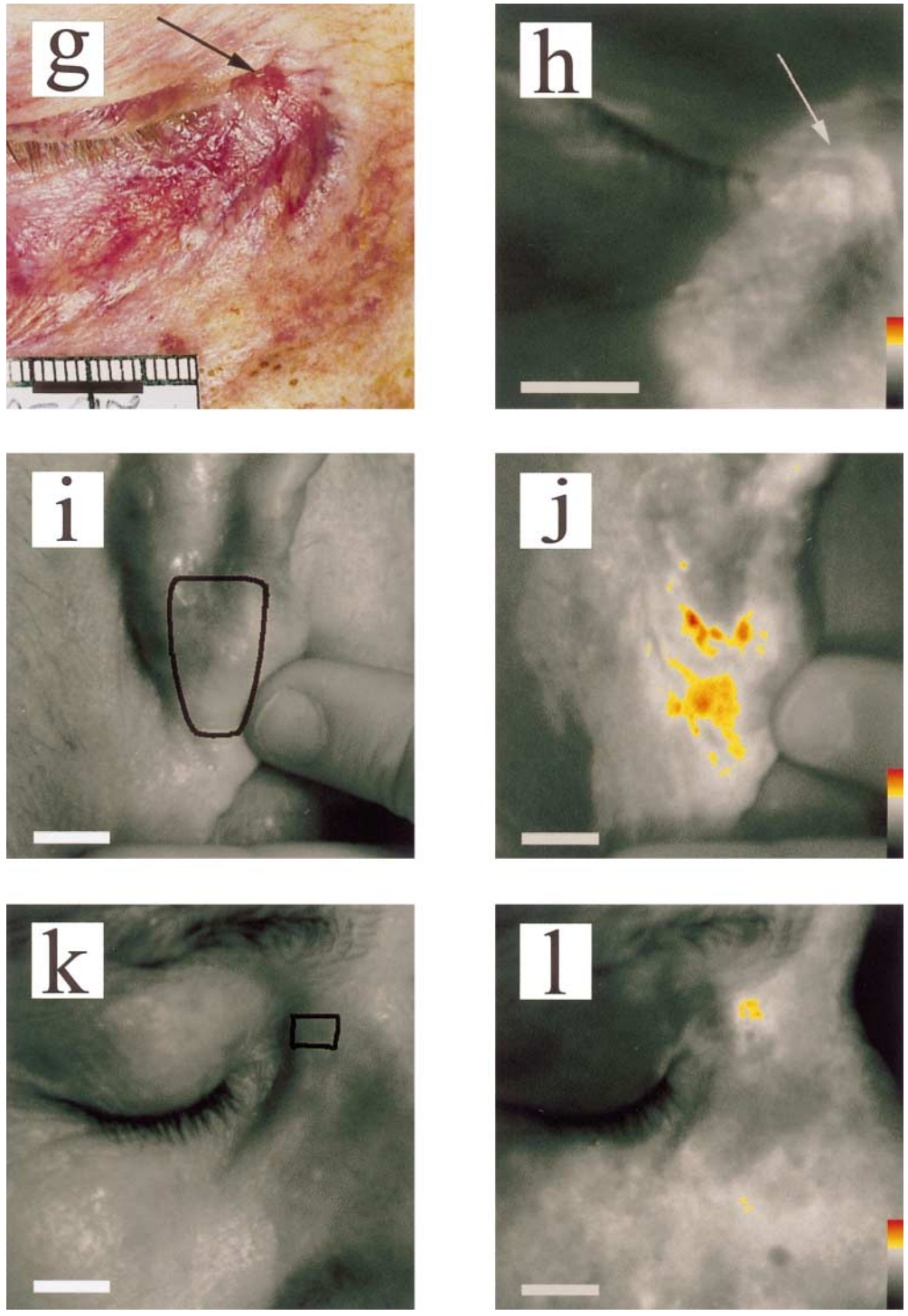

DISCUSSION

When applying fluorescence imaging to improve clinical diagnosis there are some key aspects that must be considered. These are the simplicity of the procedure, the detection limit of Pp IX and the selectivity of the method.

The imaging procedure must be simple enough to be used on a routine basis by persons not familiar with the basic principles of fluorescence imaging. The method we have developed meets this criterion as there are only three steps involved in the procedure: (i) topical ALA gel applied for 4 h; (ii) recording of a fluorescence image with the exciting light as the only light source; and (iii) analysis of the image. However, it would be desirable to reduce the time of ALA application. The detection of tumour tissue by imaging Pp IX fluorescence is based on the fact that topical application results in tissue-specific photosensitization where BCC is one type of lesion that gives rise to increased Pp IX fluorescence (6–8).

The question as to whether the Pp IX concentration is higher

in cancer cells than in normal cells has been addressed by several authors. Szumlanski et al. (13) reported higher Pp IX fluorescence from urothelial cells derived from malignancies than from normal urothelial cells exposed to ALA. Depending on genetic factors the fluorescence intensity was 9–16 times higher in the cancer cells. If we then assume that tumour cells accumulate more Pp IX than normal cells in the skin, only tissue containing a sufficient amount of tumour cells by volume can be diagnosed as being a tumour using the fluorescence detection technique. If the infiltration degree is too low, there will be too few tumour cells by volume and the signal will not exceed the natural variation of Pp IX fluorescence from normal cells and tissue fluorescence.

Martin et al. (14) reported, however, that there was no selectivity for Pp IX fluorescence in tumour tissue vs. normal skin as seen with fluorescence microscopy. They suggested, therefore, that the high external Pp IX fluorescence over tumours may be due to enhanced penetration through the stratum corneum and to the thickness of the tumour.

Szeimies et al. (15) observed a low fluorescence yield from MBBCs in a fluorescence microscopy study. In our study, we found a good correlation between the fluorescence imaging and the histological mapping in 11/22 lesions applying a strict criterion for correspondence. Some agreement (partial correlation) was found in a further 5/22 lesions. Eleven of these 22 BCCs were of morpheiform type. In 5/11 lesions we found good correlation according to the criterion and 3/11 showed partial correlation.

Factors which influence the fluorescence yield

For optimal fluorescence the application of ALA is of utmost importance. The gel should be evenly applied covering the tumour area with broad margins. The whole area should be covered with a bandage impermeable to photoactivating light. A drawback of the procedure is its inability to induce fluorescence from ulcerated tumour tissue. One possible explanation could be the lack of epithelial cells in the ulcerated area.

Another important issue is the selectivity of the Pp IX fluorescence. Kennedy et al. (5) have reported Pp IX fluorescence from sun-damaged skin, psoriasis, actinic keratoses, healing scars and normal hair follicles. This has also been seen in the present investigation.

One important fact to be taken into account when using fluorescent imaging as a diagnostic tool is that it only can demonstrate the lateral extent of a tumour as the light used for exciting Pp IX in the blue wavelength region has a poor depth of penetration in the skin (16). Thus, deep tumours that do not extend on the surface would not be detected.

The *in vivo* fluorescence imaging method presented here should be compared with the present methods for detection and delineation of BCCs, clinical experience and histology. This cross-correlation study shows that *in vivo* fluorescence imaging in many cases correlates well with histopathological examination of the excised tissue. However, further studies are needed to fully establish the predictive capability of this technique.

ACKNOWLEDGEMENTS

We thank engineer Leif Johansson, photographer Morgan Karlsson and biomedical technicians Ellinor Mattsson and Inger Roslund for their valuable help. We also thank Professor Magne Alpsten for initiating the co-operation between the Department of Physics and the Department of Dermatology. The CCD camera used in this project has been partially funded by The Carl Tryggers Foundation. The development of the imaging technique has been supported by Volvo Research Foundation and Volvo Educational Foundation (contract No. 92:36) in connection with a catalysis project. The study was also supported financially by the Welander foundation.

REFERENCES

1. Rowe DE, Carroll RJ, Day CL Jr. Long-term recurrence rates in previously untreated (primary) basal cell carcinoma: implications for patient follow-up. J Dermatol Surg Oncol 1989; 15: 315–328.
2. Marcus SL, Sobel RS, Golub AL, Carroll RL, Lundahl S, Shulman DG. Photodynamic therapy (PDT) and photodiagnosis (PD) using endogenous photosensitization induced 5-aminolevulinic acid (ALA): Current clinical and development status. Journal of Clinical Laser Med and Surg 1996; 14: 59–66.
3. Wennberg A.-M, Lindholm L.-E, Alpsten M, Larkö O. Treatment of superficial basal cell carcinomas using topically applied delta-aminolaevulinic acid and a filtered xenon lamp. Arch Dermatol Res 1996; 288: 561–564.
4. Szeimies RM, Abels C, Fritsch C, Karrer S, Steinbach P, Baumler W, et al. Wavelength dependency of photodynamic effects after sensitization with 5-aminolevulinic acid *in vitro* and *in vivo*. J Invest Dermatol 1995; 105: 672–677.
5. Kennedy JC, Pottier RH, Pross DC. Photodynamic therapy with endogenous protoporphyrin IX: Basic principles and present clinical experience. J Photochem Photobiol 1990; 6: 143–148.
6. Kennedy JC, Pottier RH. Endogenous protoporphyrin IX: a clinically useful photosensitizer for photodynamic therapy. J Photochem Photobiol B: Biol 1992; 14: 275–292.
7. Warloe T, Peng Q, Steen HB, Giercksky KE. Localization of porphyrins in human basal cell carcinoma and normal skin tissue induced by topical application of 5-amino levulinic acid. In: Spinelli P, Dal Fante M, Marchesini R eds. Photodynamic Therapy and Biomedical Lasers. Elsevier Science Publishers BV, 1992: 545–558.
8. Peng Q, Warloe T, Moan J, Heyerdahl H, Steen HB, Nesland JM, Giercksky KE. Distribution of 5-aminolevulinic acid-induced porphyrins in noduloulcerative basal cell carcinoma. Photochem Photobiol 1995; 62: 906–913.
9. Cheong WF, Prahl SA, Welch AJ. A review of the optical properties of biological tissues. IEEE J Quantum Electron 1990; 26: 2166–2185.
10. Wolff P, Rieger E, Kerl H. Topical photodynamic therapy with endogenous porphyrins after application of 5-delta-aminolevulinic acid. An alternative treatment modality for solar keratosis, superficial squamous cell carcinomas, and basal cell carcinomas? J Am Acad Dermatol 1993; 28: 17–21.
11. Svanberg K, Andersson T, Killander I, Stenram U, Andersson-Engels S, Berg R, et al. Photodynamic therapy of non-melanoma malignant tumours of the skin using topical delta-amino levulinic acid sensitization and laser irradiation. Br J Dermatol 1994; 130: 743–745.
12. Zitelli J. Mohs micrographic surgery for skin cancer. Principles and Practice of Oncology 1992; 8: 1–10.
13. Szumlanski C, Otterness D, Her C, Lee D, Brandriff B, Kelsell D, et al. Thiopurine methyltransferase pharmacogenetics: human gene cloning and characterization of a common polymorphism. DNA-Cell Biol 1996; 15: 17–30.
14. Martin A, Tope W D, Grevelink J M, Starr J C, Fewkes JL, Flotte TJ, Deutsch TF, Anderson RR. Lack of selectivity of protoporphyrin IX fluorescence for basal cell carcinoma after topical application of 5-aminolevulinic acid: implications for photodynamic treatment. Arch Dermatol Res 1995; 287: 665–674.

15. Szeimies RM, Sassy T, Landthaler M. Penetration potency of topical applied δ-aminolevulinic acid for photodynamic therapy of basal cell carcinoma. J Photochem Photobiol 1994; 59: 73 – 76.

16. Moan J, Iani V, Ma L. Choice of proper wavelength for photochemotherapy. Proceedings of Photochemotherapy and other modalities. SPIE proceeding 1996; 2625: 544 – 549.